Uncertainties in altimetry-based velocity estimates

Olwijn Leeuwenburgh and Detlef Stammer
Scripps Institution of Oceanography, University of California, San Diego, La Jolla, California, USA

Received 23 April 2001; revised 15 April 2002; accepted 22 April 2002; published 29 October 2002.

[1] Three methods to estimate ocean geostrophic surface currents from satellite altimetry measurements are evaluated for several single- and multiple-satellite configurations, with specific emphasis on resulting uncertainties. Altimetric sea surface height measurements are simulated by sampling along satellite ground tracks the surface pressure output from the 1/10° North Atlantic run of the Los Alamos Parallel Ocean Program model and by subsequently adding realistic instrument and orbit errors. The effects of both sampling and data errors on the velocity estimates are discussed. The satellite orbit configurations considered represent current missions or candidates for future coordinated tandem missions. Data error budgets are based on those of existing missions and on estimates for new altimetric technology currently under development. In midlatitude regions characterized by strong variability, such as the Gulf Stream region, velocities estimated at crossovers of interleaved tracks, and along a virtual ground track between two parallel tracks with a 0.75° zonal offset, are found to be comparable in accuracy and more accurate than velocities estimated from optimally interpolated sea surface height maps. Error variances as low as 15–25% of the local signal variance can be obtained from all three methods near the Gulf Stream core. Larger relative errors are found almost everywhere else with the exact details of the error in the two velocity components depending on data error, orbit configuration, latitude, estimation method, and smoothing. Several scientific applications of the configurations and methods are discussed, including the estimation of Reynolds stresses, momentum fluxes, velocity spectra, and covariance functions. Accuracy and applicability suggest that the newly proposed parallel track configuration is a viable option for future tandem missions. *INDEX TERMS:* 4275 Oceanography: General: Remote sensing and electromagnetic processes (0689); 4512 Oceanography: Physical: Currents; 4556 Oceanography: Physical: Sea level variations; 4594 Oceanography: Physical: Instruments and techniques; *KEYWORDS:* altimetry, volocity, Jason, TOPEX/Poseidon, SSH, accuracy

Citation: Leeuwenburgh, O., and D. Stammer, Uncertainties in altimetry-based velocity estimates, *J. Geophys. Res.*, *107*(C10), 3175, doi:10.1029/2001JC000937, 2002.

1. Introduction

[2] The ocean flow field is one of the fundamental variables in all physical and biogeochemical disciplines of oceanography. Adequate continuous sampling of the ocean's temporally and spatially highly variable state can currently only be expected from remote sensing methods, most notably satellite altimetry [*Wunsch and Stammer*, 1998]. It has been recognized, however, that a single satellite will not be sufficient to resolve the mesoscale spatial and temporal variability and that the orbit configurations of two or more satellites should be carefully coordinated in order to significantly increase the resolution toward smaller scales [*Greenslade et al.*, 1997]. This is particularly so if the aim is to estimate velocities [*Le Traon and Dibarboure*, 1999]. The prospect of future availability of multiple simultaneous altimetry missions, as well as the anticipation of new technologies, such as delay Doppler [*Raney*, 1998], Ka band [*Vincent and Thouvenot*, 2001], and wide swath altimetry [*Rodriguez et al.*, 2002], have revived the discussion about the quality of currently available sea surface height and velocity products and the achievable improvements therein. One imminent opportunity for optimal coordination of two conventional altimeters is a tandem mission of TOPEX/Poseidon (T/P) and Jason, following the initial calibration phase of Jason. It has been recommended [*Fu*, 2000] that the two satellites are flown in an "interleaved tracks" configuration, resulting in evenly spaced ground tracks, with no temporal offset. Another mission involving multiple satellites that could be optimally configured would be a WITTEX constellation of several small satellites, positioned in the same orbit plane, but separated zonally by the earth's rotation [*Raney and Porter*, 2001]. Each specific configuration might lend itself well to a particular type of velocity analysis from the sea surface

0148-0227/02/2001JC000937$09.00

height (SSH) data. In view of the existing and anticipated new multiple altimeter missions, an evaluation of accuracies of altimetric velocity estimates from all available methods is timely.

[3] Traditionally, estimates of the geostrophic surface flow field have been obtained from SSH measurements through one of two methods: space-time optimal interpolation of SSH [e.g., *Ducet et al.*, 2000], or cross-track velocity estimation at the intersection of ascending and descending tracks [e.g., *Morrow et al.*, 1994]. Different approaches have been followed in estimating and comparing the accuracies of altimetric velocities. *Le Traon and Dibarboure* [1999] considered the formal velocity errors associated with different data distributions in an application of the former method. Other studies have compared variability statistics of resulting velocities with in situ statistics obtained from drifters [e.g., *Willebrand et al.*, 1990; *Ducet et al.*, 2000]. Evaluation of velocities at crossovers has been undertaken only through fairly localized comparisons with moored current meters [e.g., *Strub et al.*, 1997].

[4] *Stammer and Dieterich* [1999] suggested an alternative approach to estimate the surface flow field, utilizing two altimeters which are operated in two identical orbits with a small zonal offset and with zero temporal offset. They devised a method, referred to here as the "parallel track method," to estimate the two orthogonal velocity components from such a configuration based on between-track differences of SSH. *Stammer and Dieterich* [1999] showed that such an observing system could, in the absence of data errors, recover the two velocity components with high along-track resolution and with adequate accuracy to produce realistic values of eddy kinetic energy and Reynolds stresses.

[5] This paper compares the ability of the above three methods to estimate surface geostrophic velocities from altimetry for several single- and multiple-satellite configurations with specific emphasis on the uncertainties associated with both sampling and data errors. Its aim is to gain a firm understanding of uncertainties in existing velocity products and establish a framework for evaluation of future tandem mission configurations. For this purpose altimetric SSH measurements were simulated from the 3 day interval output of the 1/10° North Atlantic run of the Los Alamos Parallel Ocean Program [*Smith et al.*, 2000], which contains realistic levels of SSH variability and kinetic energy on small spatial scales. The effects of data errors on velocity estimates were studied by adding random noise and orbit errors with realistic magnitudes to the SSH measurements. Since all measurements are based on the same source and are being analyzed over the same regions, this analysis will allow an objective comparison of the performance of the respective configurations and methods, and will provide a quantitative error analysis of previous and future studies of the ocean flow field based on altimetric data.

[6] M. Schlax and D. B. Chelton (The accuracies of crossover and parallel-track estimates of geostrophic velocity from TOPEX/Poseidon and Jason altimeter data, submitted to *Journal of Geophysical Research*, 2002, hereinafter referred to as Schlax and Chelton, submitted manuscript, 2002) developed analytical expressions for velocity errors from parallel track and crossover methods associated with instrument noise and long-wavelength data errors, and investigated the filtering characteristics of the applied data processing methods. In this paper the joint effect of data and sampling errors on velocity uncertainties are considered. The importance of spatial and temporal sampling characteristics is illustrated in Figure 1 showing the fraction of model kinetic energy reproduced for two different SSH sampling cases. In case (a) SSH samples were selected from a 0.8° subgrid of the model to calculate the slopes. The distances between SSH samples vary significantly with latitude but compare roughly with the scale of the mesoscale eddy field (see Figure 2). In this case more than 70% of the total model eddy kinetic energy is reproduced almost everywhere, except in the subpolar gyre. In contrast, in case (b), where slopes are evaluated from model SSH samples separated by 1.8°, no more than 50% of eddy kinetic energy is captured anywhere in the extratropical Atlantic. This clearly illustrates the importance of resolving the small spatial scales in studies of the variability of the flow field. A similar need to resolve variability on small

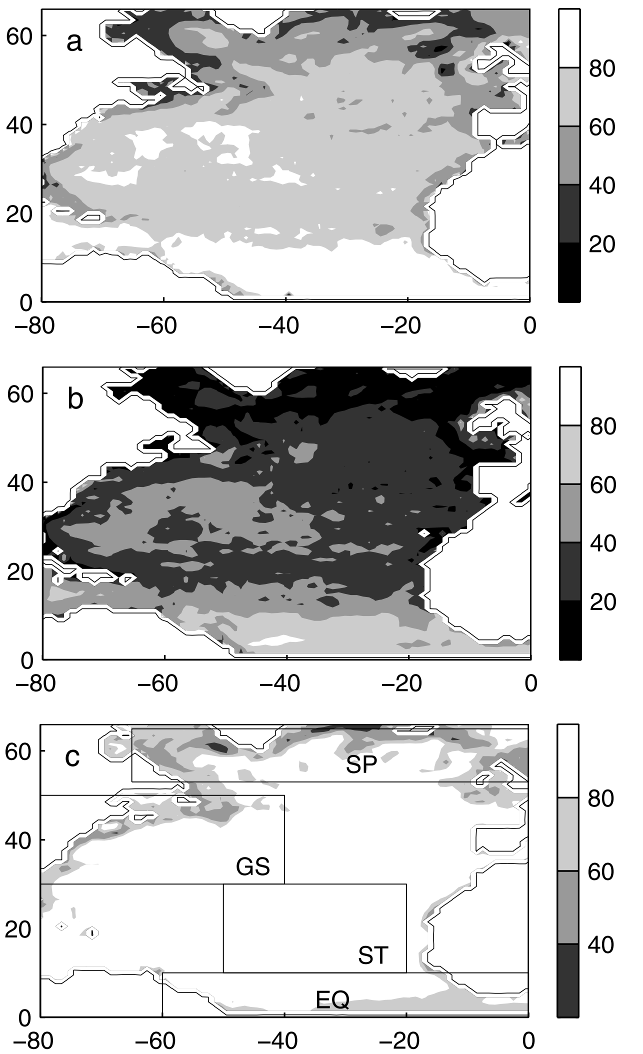

Figure 1. (a) and (b) Fraction of model eddy kinetic energy reproduced from model SSH samples separated by the distances a and b depicted in Figure 2, as explained in the text; (c) fraction of model kinetic energy on timescales longer than 20 days.

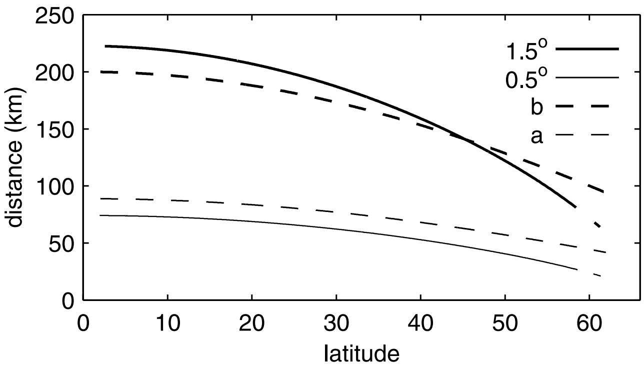

Figure 2. Distance between model SSH samples used in Figures 1a and 1b and between SSH samples as obtained from the parallel track method for track separations of 1.5° and 0.5°.

timescales is illustrated in Figure 1c, showing the fraction of eddy kinetic energy on timescales longer than 20 days, the shortest period that can be resolved from sampling at a repeat interval similar to that of T/P. Both along the ocean margins and at high latitudes, a significant fraction of kinetic energy is located in the high-frequency band before *Stammer et al.* [2000] relate the variability in the subpolar North Atlantic to wind-induced barotropic motions). This may affect velocity estimates obtained from sampling strategies that do not properly resolve these timescales.

[7] The structure of the remainder of this paper is as follows. Section 2 revisits the parallel track method, and its ability to observe the ocean velocity with and without data errors, for two T/P-like satellites in orbits with offsets between 0.25° and 1.5°. Sections 3 and 4 will provide similar considerations for the crossover method and optimal interpolation. These two methods are applied to data from two T/P-like satellites in the interleaving configuration, as well as from several alternative satellite constellations. The applicability of these configurations and methods to scientific investigation is discussed in section 5. Section 6 finally ends with a summary and conclusions.

2. Two Altimeters in Parallel Tracks

2.1. Method

[8] The approach taken here is similar to that of *Stammer and Dieterich* [1999], who presented a schematic of the construction of SSH slopes and subsequent calculation of velocities in two orthogonal directions using observations from two parallel tracks. Following their suggestion, spherical geometry was applied here. Model velocities were obtained on the model grid by taking centered differences over 0.2° of the model SSH. Along-track SSH, as well as between-track velocities were then obtained through bilinear interpolation using the surrounding four model grid points.

[9] The results obtained by *Stammer and Dieterich* [1999], although promising, have limited applicability for two distinct reasons. First, SSH measurements were simulated using a 1/3° model which fundamentally underestimated the kinetic energy on small spatial scales as compared to that observed in the ocean. The presence of increased small-scale variability may alter the results due to the dependence of the accuracy of the velocity estimates on the zonal separation between the two altimeter tracks. A track separation which exceeds the spatial scales of energetic sea surface height variability will lead to an aliasing of energy into larger spatial scales. Second, only error-free observations were considered. Since the estimation of velocities is based on between-track gradients of SSH, any errors in the SSH data that result in random or systematic biases between the two tracks may lead to large velocity errors. Both of these factors potentially lead to an overly optimistic assessment of the method.

[10] A first insight into the sensitivity to track separation and the resulting sampling error is obtained by considering the distances over which slopes are computed. As can be seen in Figure 2 the distance between selected samples of SSH varies significantly with latitude for any fixed zonal track separation. A track separation of 1.5° will mean that slopes are estimated over distances ranging from 225 km near the equator to 75 km at 60° latitude. For a track separation of 0.5°, the distance between samples ranges from 75 km at low latitudes to 25 km toward the turning latitude. It is quite fortunate that this range in distances over which SSH slopes are evaluated is similar to the change with latitude of spatial eddy scales [*Stammer*, 1997]. If spatial aliasing is to be avoided, these distances between SSH samples should not exceed those typical spatial scales of variability at any latitude. As shown in Figure 2, the two examples of track separation correspond closely to the two cases considered in Figure 1, with a 1.5° separation leading to severe under estimation of mesoscale ocean variability. This would suggest that application of the parallel track method of velocity estimation must be excluded as a quantitatively satisfying option for configurations with large track separations (the 1.5° track separation is identical to an interleaved tracks scenario).

[11] An important benefit of the parallel track method, besides its high-density along-track measurement of the flow field, is the fact that both components of the flow field are sampled instantaneously such that errors related to the temporal sampling can be neglected (see the discussion on the crossover method below). Therefore it was assumed here for computational convenience that a complete set of tracks is measured during each 3 day model frame.

2.2. Sampling Errors

[12] In order to assess the sampling-imposed limitations of an observing system consisting of two satellites operating in slightly offset orbits, no data errors were applied at first. Any resulting velocity errors can thus be ascribed entirely to inadequate spatial sampling. These calculations also serve to test the conclusions reached before by *Stammer and Dieterich* [1999] from less realistic model simulations. As will be shown below, these conclusions remain valid when using the Los Alamos model.

[13] Sampling errors are summarized in Figure 3 in terms of error-to-signal variance ratios (in percentages) for four dynamically distinct regions as a function of track separation. These regions are indicated by the boxes in Figure 1c. In all four regions the differences between the 'true' and estimated velocities tend to decrease with track separation suggesting that the smallest possible track separation is the

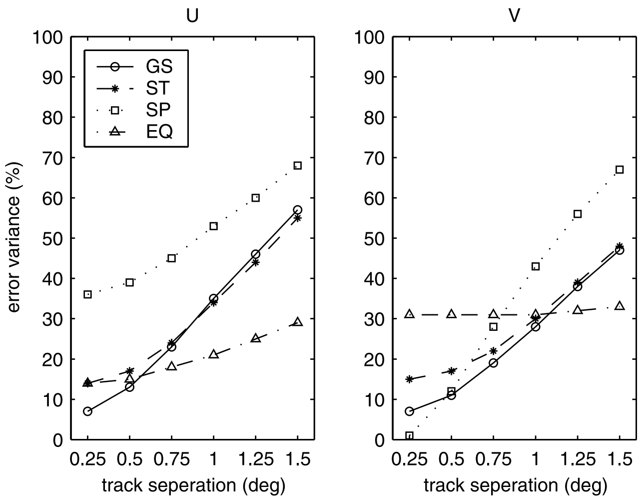

Figure 3. Sampling error variances expressed as a percentage of local signal variance for *U* and *V* as obtained from the parallel track method for several track separations in four geographical regions: 30°–50°N, 80°–40°W (GS), 10°–30°N, 50°–20°W (ST), 53°–66°N (SP), and 0°–10°N (EQ).

preferred configuration for application of this velocity estimation method. It can also be seen that in both the GS and ST regions the *U* and *V* components are retrieved with comparable accuracy and that error variances increase from 10% to 50% of the signal variance when the track separation is increased from 0.25° to 1.5°. At latitudes between 10° and 30° the *V* component can be particularly well determined for very small track separations. Close to the equator on the other hand the error variances of the *V* component never decrease below 35% of the signal variance. At high latitudes similarly unrealistic values are obtained for the *U* component. The large velocity errors at the smallest track separation in these two cases originate in the various interpolation and approximation steps involved in the estimation procedure, leading to small errors in the data. The strong sensitivity of *U* and *V* to data error associated with small scales and the $1/f$ factor at high and low latitudes respectively becomes more obvious when noise and orbit errors are introduced, as is done in the next section, and the effects of interpolation error will turn out to be negligible in comparison.

2.3. Data Errors

[14] Unlike the ideal case described in the previous section, altimeter observations contain uncertainties due to instrument noise and contributions from orbit errors, geophysical effects (especially electromagnetic bias), and environmental effects, such as those associated with atmospheric water vapor.

[15] Instrument noise arises from errors in the measurement of the travel time of the radar pulse and has a random character. These errors were simulated here by Gaussian distributed random noise with zero mean. For the standard deviation values of 1 cm and 2 cm were assumed. The 2 cm standard deviation is a realistic value for TOPEX class altimeters [*Chelton et al.*, 2001], whereas 1 cm might be achieved from new techniques such as delay Doppler or Ka band altimetry. Most of the geophysical and environmental errors are of the same spatial scale as atmospheric disturbances and will largely cancel in the differences between two closely positioned satellite tracks. Orbit errors have little effect on along-track slopes but introduce a bias when slopes are computed between neighboring tracks. A similar type of bias may result from an incomplete calibration of sensors on board the two satellite busses. Orbit errors were simulated by a once-per-revolution cycle with an amplitude of 1 to 3 cm and random phase shift between repeats. Although not explored here, orbit errors can be reduced to a certain extent by minimizing SSH differences between tracks at crossovers [e.g., *Knudsen*, 1993]. This is particularly effective for two satellites positioned in two orbits with a small spacetime offset, or in the same orbit as in a WITTEX constellation, when applied near the turning latitude (R. K. Raney, personal communication). Since the time difference between the two measurements in this case is practically negligible, the minimization will be much more efficient than for a single satellite or a pair of satellites in different orbit configurations.

[16] The lateral departure of the ground track from the reference path (generally kept below ±1 km) introduces an error in the sea level anomaly in proportion to the cross-track mean sea surface slope. The mean sea surface slope is strongly affected by the presence of steep bottom features such as sea mounts and has similar spatial scales. For example, *Høyer et al.* [2002] find local slopes of up to 10 cm/km in the mean sea surface at the Charlie-Gibbs and Romanche Fracture Zones. A ground track displacement in the presence of a cross-track slope introduces an error in the slope between neighboring tracks which cannot be removed by along-track smoothing and which, if uncorrected, may therefore lead to errors in the velocity estimates obtained from this method. Since the along-track wave number spectrum of these errors is not known in detail, two different forms were considered: a uniform bias and random noise, in both cases added to one of the two tracks after any along-track smoothing. It is assumed in the following that all such errors are collectively of order 1 cm for each pair of SSH observations. This type of error can possibly be reduced with the use of improved cross-track geoid gradient estimates (D. Chambers, personal communication), but no attempt was made here to simulate these kinds of procedures.

[17] It is known that there is small-scale sea level variability that can be associated with internal tides [*Ray and Mitchum*, 1996]. Such signals may be on the order of a few centimeters near major bathymetric features, but are mostly smaller. No attempts were made here to simulate and remove these signals.

[18] Truly random noise can be substantially suppressed through along-track smoothing of the SSH measurements. However, the smoothing parameters need to be chosen carefully, such that the noise is effectively reduced but without inadvertently removing a significant fraction of the SSH and velocity signal which one attempts to study. It is therefore worthwhile to recall that the ocean eddy field exhibits spatial scales that fundamentally depend on geographic position and primarily decrease toward high latitudes [e.g., *Stammer*, 1997]. In order to account for varying eddy scales and obtain a sufficient noise suppression, the

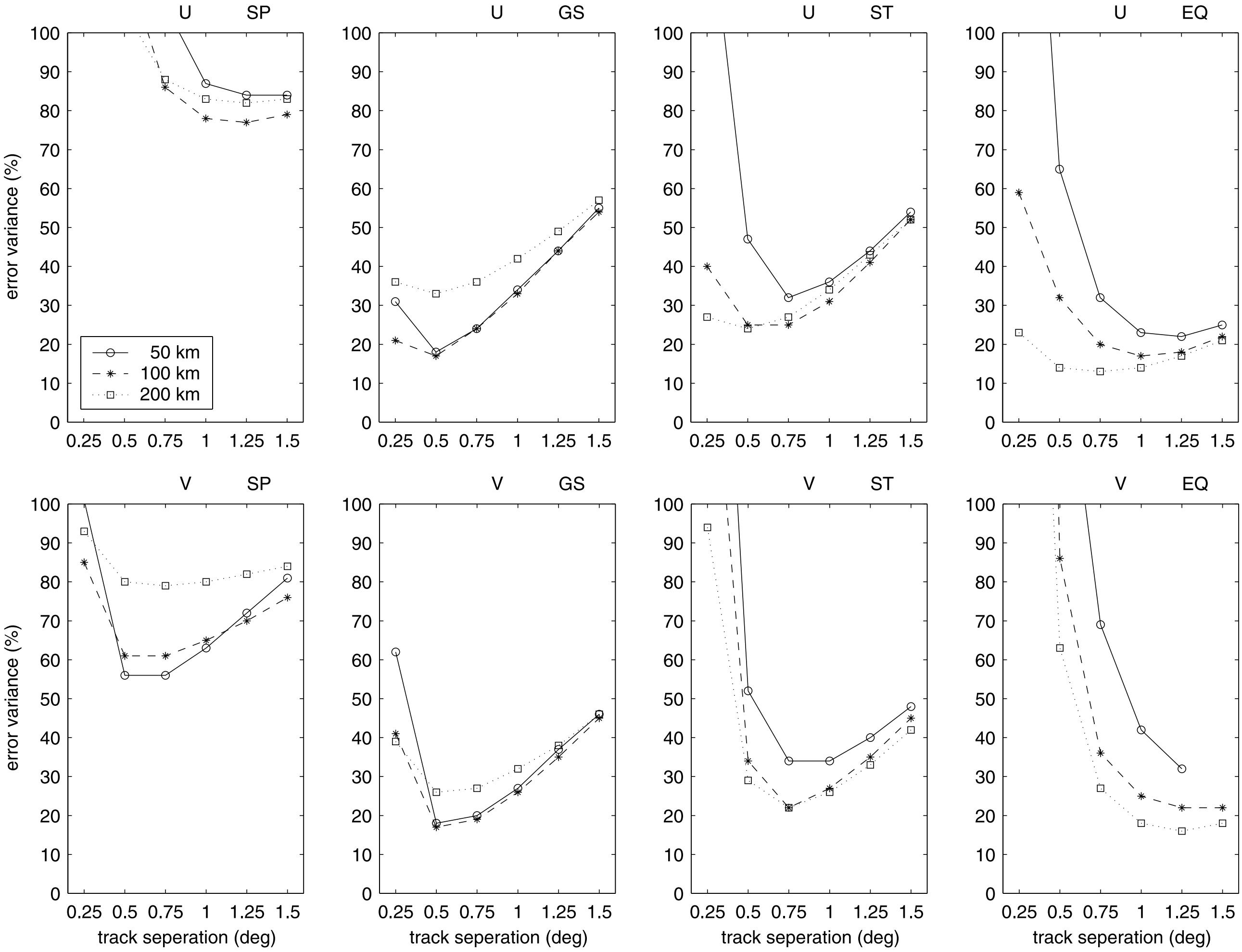

Figure 4. As in Figure 3 but for 2 cm instrument noise and with 50, 100, and 200 km smoothing.

effect of several smoothing length scales was tested for each of the track separations and geographical regions considered in the previous section (Figure 4). In this case 2 cm noise and 2 cm orbit errors were added to the simulated data which were subsequently smoothed by applying a quadratic loess smoother [*Cleveland and Devlin*, 1988; *Schlax and Chelton*, 1992] with cutoff wavelengths of 50, 100, and 200 km. Clearly the dependence of velocity errors on track separation is quite different from the ideal case in that the accuracies of velocity estimates obtained for very small track separations are now severely affected by data errors. In some cases, such as for the *U* component at latitudes above 53°, and the *V* component at latitudes below 10°, the error variance may become larger than the signal variance. Since the velocities are calculated from SSH gradients between two noisy measurements, the effect of data errors will be increased if the distance between the two points is decreased. This contrasts the result from the ideal case in that now the smallest track separations do not lead to the best results. However, for the GS and ST regions results are still similar to the ideal case for larger track separations, suggesting that the impact of data errors is reduced when gradients are taken over larger distances while spatial sampling errors are enhanced and start to dominate.

[19] Because of the dissimilar impacts of data and sampling errors, the choice of smoothing length scale is of critical importance. For the two low-latitude regions a smoothing length scale of 200 km leads to the best results, while at middle and high latitudes a smoothing length scale of 100 km is to be preferred. These smoothing scales are used in Figure 5 where different error scenarios are considered, based on the discussion above. The cases with 2 cm noise and 2 or 3 cm orbit error are representative of a T/P class altimeter. The 1 cm noise cases are supposed to represent the delay Doppler and Ka band types of altimeters currently under development. As discussed earlier, a 1 cm orbit precision may possibly be achieved by crossover minimization for multiple satellites in coordinated orbits.

[20] For T/P-like tandem missions, high accuracy in both components is only achieved in the GS region where error variances of roughly 35% can be obtained with a 0.75° track separation (Figure 5). However, even with a 3 cm orbit error useful velocity estimates can still be obtained. In all other regions one or both of the components are severely corrupted by data errors and, to a lesser extent, sampling problems. Significant improvements, especially in the *V* component, are made if the orbit error can be reduced to 1 cm, which would enable application of the method to equatorial and subtropical regions. Even though for this optimistic error

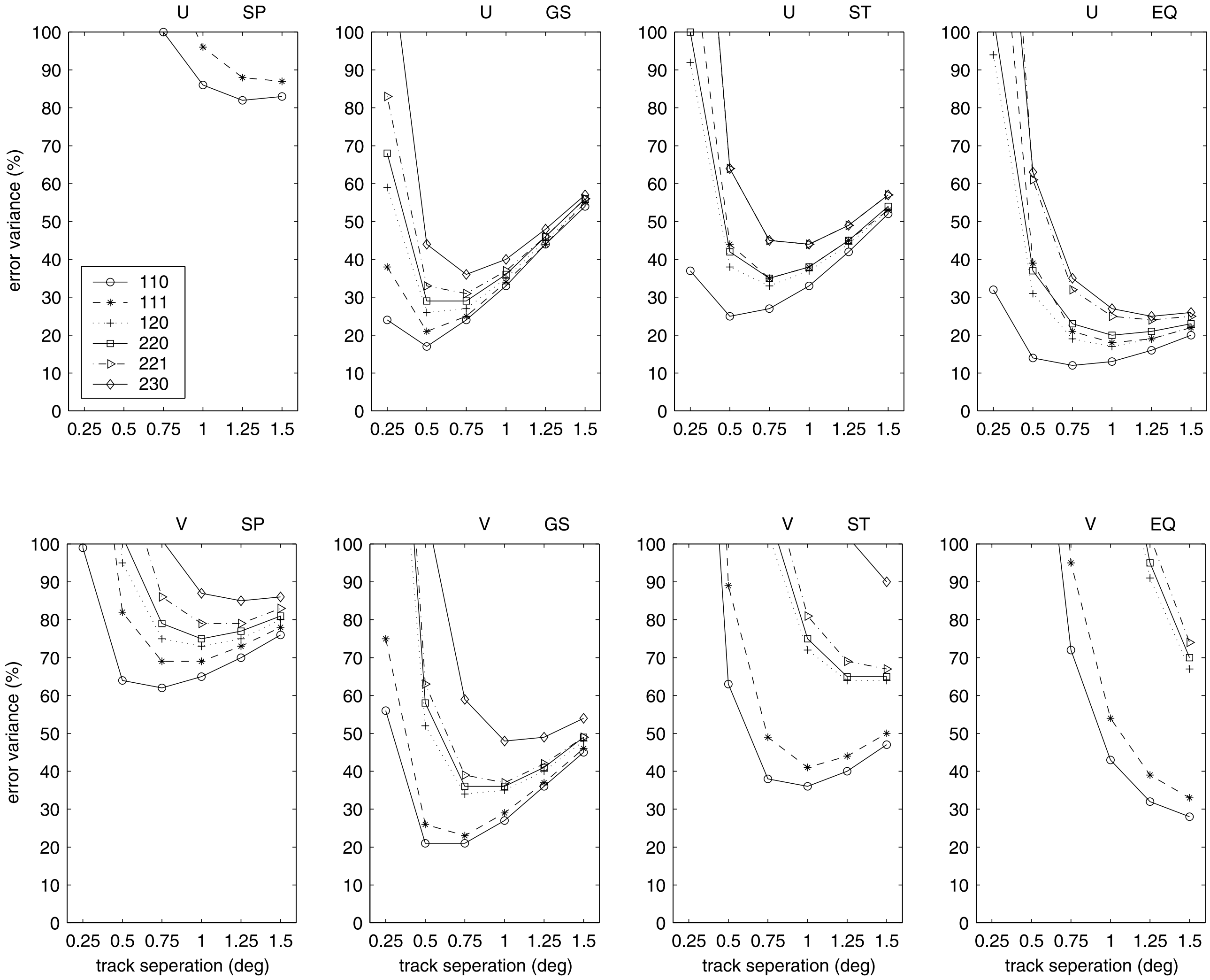

Figure 5. As in Figure 3 but for different data error budgets with individual components representing (from left to right, in cm) instrument noise, orbit error, and random bias. In the SP and GS regions, along-track smoothing with a 100 km wavelength cutoff was applied, while in the ST and EQ regions, 200 km was used.

budget the choice of track separation is less crucial than for the other cases, an optimum configuration can still be determined. In comparison to the improvements obtained from a 1 cm reduction of orbit errors or other biases, a 1 cm noise reduction does not have a large impact. The addition of a 1 cm random along-track bias raises uncertainties significantly in most areas but has only little effect in the GS region. The impact of adding a uniform 1 cm along-track bias is generally comparable to increasing the orbit error by 1 cm (not shown).

3. Velocity Estimation at Crossovers

3.1. Method

[21] At crossover locations where ascending and descending arcs intersect, it is possible to estimate two components of the velocity vector, which subsequently can be rotated into a Cartesian reference frame. The uncertainties in the resulting eastward and northward velocity components depend both on data errors and on the angle between the ground tracks and the north meridian [*Parke et al.*, 1987; *Morrow et al.*, 1994]. In addition, the two components are not obtained simultaneously, but with a time lag. This time lag between over flights on crossing arcs is a function of latitude [cf. *Morrow et al.*, 1994, Figure A1] and may be as large as half the repeat period (4.8 days for a T/P-like mission). This forms a third source of error in the velocity estimates, whose magnitude depends jointly on the length of this time lag and on the timescale of ocean variability at the crossover location. This means that a realistic simulation of the temporal sampling of SSH is required for proper examination of the resulting velocity uncertainties.

[22] The interleaved-tracks scenario with no time offset was investigated for a tandem T/P-Jason mission. The addition of a second satellite will double the number of both ascending and descending arcs and thus quadruple the number of crossovers. For comparison, additional simulations were performed for single-satellite ERS (Envisat) and Geosat (GFO) orbit configurations, both of which are characterized by a much denser coverage of crossover

points as compared to just the single T/P mission, but also by a substantially longer repeat period and thus by a longer maximum time lag at crossovers.

[23] The methodology applied here was chosen to replicate the data processing steps that one would take in dealing with real altimetric data. First, observations were simulated along all arcs for every 3 day model frame using the model SSH output. These observations were then linearly interpolated to the sampling times of an actual altimeter. In this way both the spatial and temporal sampling characteristics of the altimeter mission were reproduced. By determining the slope of a straight line, fit to these simulated along-track observations at each crossover location, time series of cross-track velocities at the overflight times were constructed for both ascending and descending arcs. These two time series were then linearly interpolated to a common time. To minimize the temporal sampling error this time was taken to be the midtime between the two over flights [*Morrow et al.*, 1994]. Subsequently, the two velocity components were rotated into a local north and east oriented Cartesian frame. The estimation times, as well as the crossover positions, were used to obtain the corresponding 'true' velocities from the model.

[24] Using this setup, the effects on velocity estimates of data errors, smoothing length scales, temporal sampling, crossover angle, and of a time offset between the two missions are investigated. Instrument noise in the altimetric data will affect the estimation of the along-track SSH gradient and thus of the velocity at the crossover points. The advantage of crossovers, however, is that since SSH observations from a single track only are used, the method is not sensitive to biases between tracks and thus not seriously affected by orbit errors, which are therefore not explicitly considered here. The zonal track separation for the interleaving T/P-Jason scenario is 1.417 degrees, or 157 km at the equator (80 km and 164 km for Envisat and GFO, respectively). At 60°N this distance is reduced to half that value.

3.2. Sampling Errors

[25] In order to investigate the sampling limitations of this method, the ideal case in which no data errors are present is again considered first for an interleaved T/P-Jason combination. Figure 6 displays errors in the *U* and *V* components separately for the four geographical regions considered in the previous sections as a function of the span over which a straight line is fit to the along-track data. An increasing span imposes a progressively enhanced implicit smoothing on the velocity data. It is therefore not surprising that in the noise-free case (indicated by the line labelled T/P 0) the highest velocity accuracies are obtained for small spans of the fit. The influence of the crossover angle is indicated by the fact that the *U* component can not be resolved with adequate accuracy at high latitudes (errors are larger than the signal) whereas the *V* component is very poorly resolved at low latitudes. The temporal variability of the ocean on short timescales imposes a limit on the achievable accuracy of the velocity components. This is particularly clear for the GS region where the *V* component has a minimum error variance of 20%, although the accuracy of the *U* component is less constrained here.

[26] The interleaving tracks scenario does in principle allow a time offset between the two missions. In order to test the impact of such a time offset, we repeated the above calculation for the T/P-Jason tandem configuration after introducing a 4.8 day time offset (half a repeat period) between the two altimeters. It was found that only small differences in errors occur in narrow latitude bands, reflecting a latitudinal shift of the crossover time lag function. No general improvement was observed however when averaged over geographical regions of the extent considered here and we conclude that a time offset between the two interleaving altimeters will not lead to an overall velocity error reduction.

[27] The above calculations were also repeated for the Geosat (GFO) and ERS (Envisat) missions, in both cases for a single-satellite configuration. These satellites operate in 17 day and 35 day repeat orbits respectively, as compared to the 10 day T/P repeat, with inclinations of 108° and 97° respectively, as compared to the 66° inclination of T/P. Both Geosat and ERS (not shown) configurations lead to similar velocity sampling errors in the *U* component, while the accuracy in *V* is distinctly lower for these missions (in case of an ERS configuration, the *V* component can only be determined in the ST region, with relative error variances larger than 70%). The error level is generally higher for these two missions than for T/P, reflecting the influence of longer time lags between ascending and descending over flights at crossover locations. The higher inclinations of these orbits make it possible to resolve the *U* component at high latitudes but at the same time limit the accuracy of the *V* component, particularly in the case of an ERS-type configuration. The inclination and repeat period of an ERS-type mission by itself are too restrictive for velocity estimation.

3.3. Data Errors

[28] As mentioned earlier, velocity estimates obtained at crossovers are insensitive to long-wavelength data errors such as orbit and environmental errors. The slope at a crossover will be affected by noise however. Instrument noise can be repressed through along-track smoothing which is represented here by increasing the number of along-track samples used in the least squares fit of a straight line. Schlax and Chelton (submitted manuscript, 2002) give expressions for the spatial resolution of the resulting velocities. Ground track displacements may affect the slope as well to the extent that the resulting SSH errors have a short-wavelength along-track component. This case was simulated in the section on the parallel track method by adding 1 cm random along-track variability after smoothing. For the crossover method one could consider increasing the instrument noise level. No attempts were made here to account for this type of error but could be considered in regions of steep bathymetric features.

[29] Figure 6 shows velocity error variances for a tandem T/P-Jason mission with 1 and 2 cm noise, and for a single Geosat mission with 4 cm noise [*Chelton et al.*, 2001]. The uncertainties are highly sensitive to the extent of smoothing, as parameterized by the span of the least squares fit, with a clear error minimum appearing for each region. For a 10 day repeat mission like T/P with 2 cm noise, the optimal span is found to be 100 km (about 16 along-track samples) at the latitudes of the Gulf Stream and Subtropical

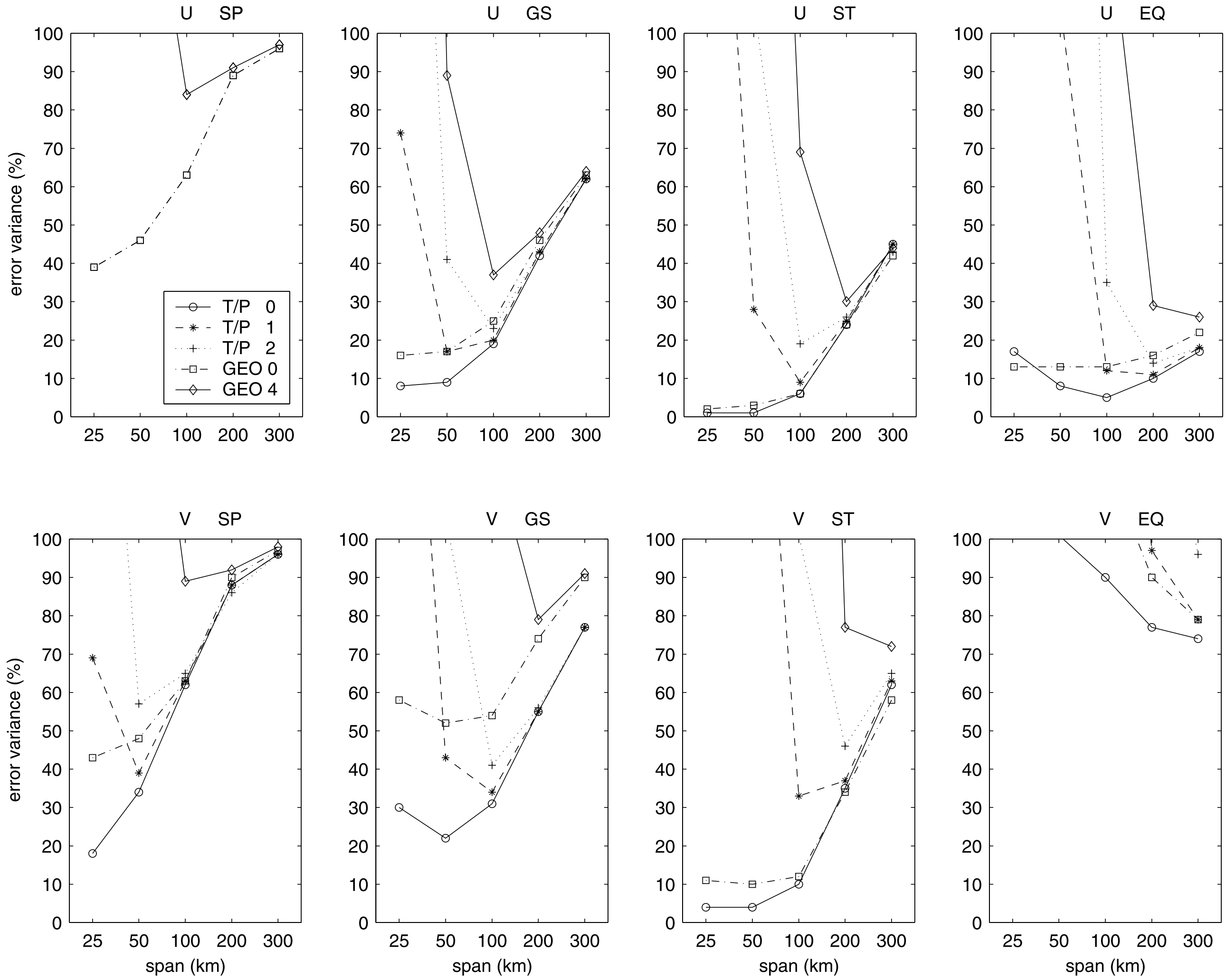

Figure 6. Error variances expressed as a percentage of local signal variance for *U* and *V* obtained from the crossover method applied to the tandem T/P-Jason (T/P) and single Geosat (GEO) missions in four geographical regions for several data error scenarios and as a function of the span of the least squares fit.

Gyre, resulting in error variances of 20% and 40% for the *U* and *V* components respectively. At high latitudes the *V* component can be estimated with a span of 50 km but the *U* component remains unresolved (the error variance is larger than the signal variance). A span of 200 km would resolve the *U* component at the lowest latitudes, but not the *V* component.

[30] For realistic error budgets reflecting the higher instrument noise levels of the Geosat and ERS missions, high accuracies can not be obtained for both velocity components simultaneously when averaged over the geographical regions considered here. A Geosat-like mission however would benefit from lower instrument noise than was available for the Geosat mission itself.

4. Optimal Interpolation

4.1. Method

[31] Optimal interpolation (sometimes referred to as objective mapping) is the preferred method to obtain SSH fields on regular space and time grids. Furthermore, the optimal interpolation procedure provides formal estimates of uncertainties, which can be studied as part of an observation system design exercise. The method of obtaining velocities from optimal interpolation roughly consists of two main steps: first, along-track SSH measurements are mapped onto a regular grid using space-time interpolation, and second, horizontal velocity components are calculated from SSH gradients in north–south and east–west directions. Alternatively, the velocities can be mapped directly from SSH using the cross-covariance functions between SSH and the two velocity components. In this paper the former approach is adopted.

[32] Application of the optimal interpolation method to velocity estimation was explored in much detail by *Le Traon and Dibarboure* [1999]. They presented formal mapping errors in *U* and *V* as a percentage of local signal variance for a range of spatial and temporal correlation scales, two different latitude bands, and a variety of mission combinations. *Ducet et al.* [2000] used optimal interpolation to obtain global velocity maps from T/P and ERS data. As a complement to these experiments, and for comparison with the results obtained in the previous sections, uncertainties in *U* and *V* are investigated here for a T/P-Jason interleaving

tandem configuration, a T/P-ERS (or similarly, Jason-Envisat) combination, a T/P-ERS-Geosat (Jason-Envisat-GFO) combination, and for a coordinated three-satellite WITTEX constellation in the T/P orbit.

[33] Although conceptually simple, in practice one encounters many practical problems. For one, optimal interpolation is computationally expensive. Also, it requires an estimate of the covariance functions of the SSH field and of the data errors. Since one or both of these are sometimes poorly known, some assumptions and approximations are usually made (it should be pointed out here that similar knowledge or assumptions are used when choosing the extent of along-track smoothing as applied in the previous sections).

[34] Since in this case the model, which contains no measurement errors, provides the true signal covariance function, it is possible, in principle, to estimate a truly optimal solution. With this in mind, zonal, meridional and temporal *e*-folding scales of SSH variability were calculated directly from the model output for each of the four geographical regions considered previously. These scales were used along with the local signal variances in an anisotropic spatial-temporal Gaussian covariance model. In the SP region an exponential temporal decay was found to be more appropriate. (It might be possible to find more optimal covariance models for smaller subregions, leading to locally better mapping results. The objective here however is the optimum for the entire region). From each of the four spatial quadrants surrounding each estimation point, the four nearest along-track SSH data points were selected for each mission separately. While limiting the number of points used, this ensures that their distribution is more or less equal in all directions, thus avoiding that all points lie on one side of the estimation point only. From each of these sample locations, all observations made within roughly 30 days (longer than the estimated *e*-folding scales) of the interpolation time were used to estimate SSH on the 1/10° model grid. The accuracies of the interpolated SSH maps were compared to those of *Le Traon et al.* [2001], who used the same numerical model to investigate the uncertainties in maps of SSH. Even though they did not incorporate orbit errors, their results were found to agree well with those obtained here. The next step was to obtain velocities by calculating the SSH slope from the least squares fit of a straight line, similar to the approach taken in the application of the crossover method. By adjusting the span of the fit one again imposes a varying degree of smoothing on the SSH mapping error and on the velocity estimates. The spans that were used here are identical to those used earlier and vary from 25 km to 300 km. One may additionally consider using the formal SSH mapping errors to supply weights to the least squares fitting procedure, but this approach has not been pursued here.

4.2. Sampling Errors

[35] Initial computations were carried out again using simulated data without data errors. To ensure nonsingularity of the SSH data covariance matrix, a small 'noise' variance term was added to the diagonal. Velocity estimates were obtained by estimating the SSH slope over varying length spans as described above. The resulting velocity errors represent the impact of the irregular spatial and temporal data distribution. Figure 7 summarizes the results for the four geographical regions. For all four combinations velocity errors are fairly similar in the two components. Up to midlatitudes uncertainties in V are generally only slightly larger than those in U, while the reverse is observed in the SP region. This is due to the latitude-dependent relative sensitivity of the two components to the ground track azimuth. In the subtropical gyre the smallest errors are generally obtained with a span of 100 km, while at near-equatorial and high latitudes longer (200–300 km) and shorter (50 km) spans respectively lead to a higher accuracy. The error curves tend to converge for longer smoothing spans, implying that longer spatial scales are equally well resolved from all four mission combinations, with SSH mapping errors related to data noise effectively being eliminated. Velocity errors increase toward higher latitudes with the largest uncertainties being found at subpolar latitudes, amounting to about 75% or more of the signal variance. Unlike the velocities obtained from the previously discussed methods, this behavior is observed in both U and V components. In the GS region the average velocity uncertainty associated with sampling errors is approximately 45% in both components for a T/P-Jason combination, and about 50–55% for a T/P-ERS combination. The three-satellite Jason-Envisat-GFO combination leads to slightly better results than an interleaved T/P-Jason tandem mission in this case. A coordinated three-satellite combination would improve the accuracy of velocity fields only in the subtropical gyre.

[36] Velocity errors are generally higher than estimates of formal mapping errors [cf. *Le Traon and Dibarboure*, 1999]. *Le Traon et al.* [2001] ascribe a similar difference in the SSH mapping errors to high-frequency and high-wave number signals present in the model, which are not properly represented in the covariance function and not resolved from the interpolation. However, the relative mapping capabilities of the different mission combinations are consistent with the results based on formal errors, implying that the velocity errors obtained from mission combinations which are not considered in this paper can easily be deduced.

[37] Some improvements can possibly be made over these results. In areas with strong planetary wave signatures, accounting for westward propagating signal in the covariance function can be shown to reduce the formal SSH mapping error. *Kuragano and Kamachi* [2000] also found some improvements in SSH maps obtained from T/P altimetry after comparison with tide gauge data. This approach was not investigated here.

4.3. Data Errors

[38] Similar to the previous sections, instrument noise was assumed to have a standard deviation of 2 cm for T/P and Jason, 3 cm for ERS, and 4 cm for Geosat. Orbit errors of 2 cm were applied to T/P, Jason and WITTEX data, and 4 cm orbit errors were assumed for ERS and Geosat. Rather than applying any along-track smoothing, which would affect the SSH covariance structure, the noise was accounted for by adding a variance term to the diagonal elements of the data covariance matrix. This in effect reduces the correlation between neighboring data samples. In contrast, the effect of orbit errors is rather to increase the correlation between two samples on the same track and

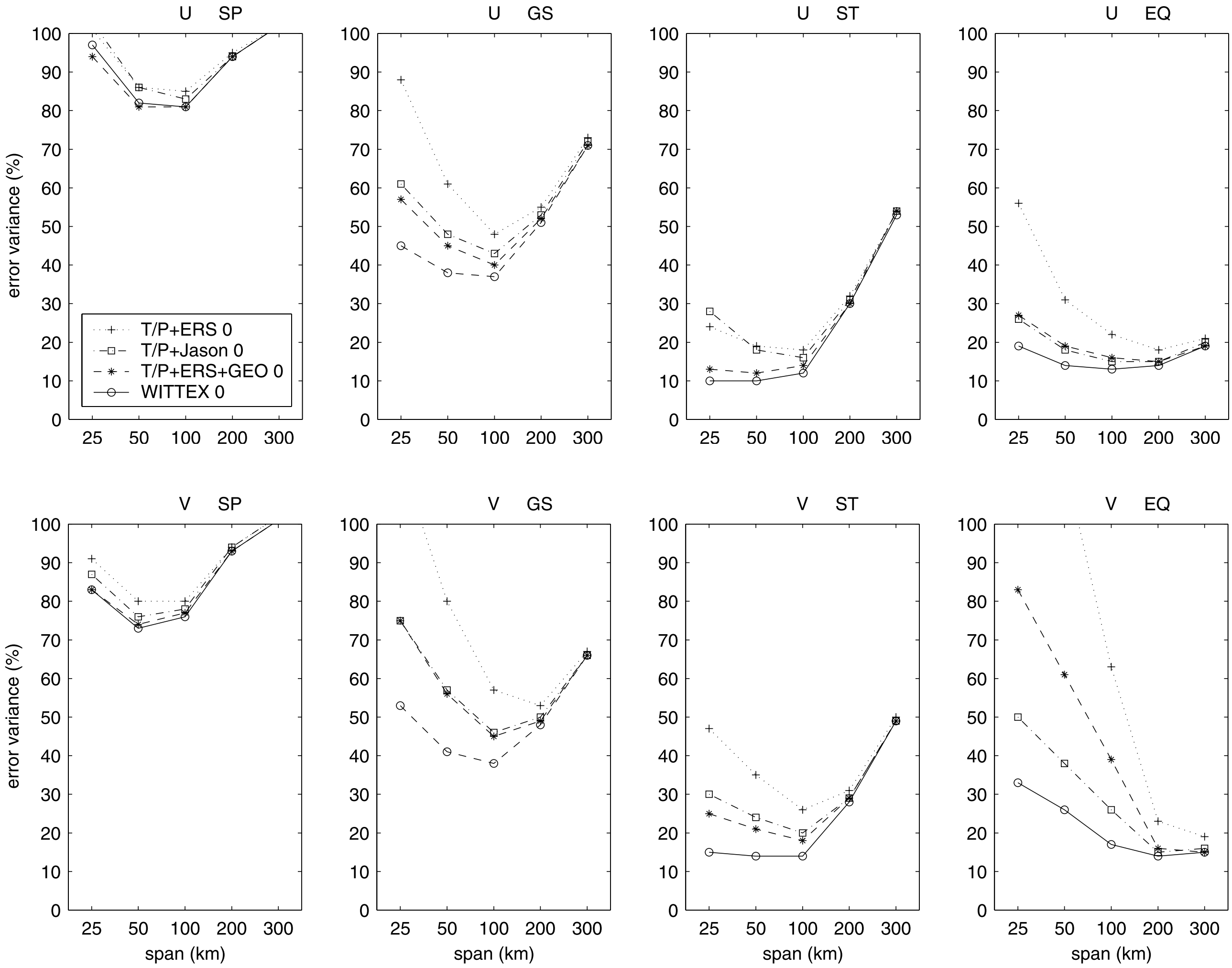

Figure 7. Error variances expressed as a percentage of local signal variance for *U* and *V* obtained by the optimal interpolation method applied to the T/P-Jason, T/P-ERS, T/P-ERS-Geosat, and three-satellite WITTEX combinations in four geographical regions as a function of the span of the least squares fit.

within the same repeat. Therefore an orbit error covariance model was applied here with an along-track correlation scale of 7000 km.

[39] The results for the cases with data errors are shown in Figure 8. It appears that the presence of data errors has a different effect in GS and SP regions as compared with the ST and EQ regions. While data errors seem to contribute little to the total velocity uncertainties in the former regions, velocities are notably affected in the latter. Velocities in the ST region are more sensitive to instrument noise and orbit error because of the relatively low signal variability, while the $1/f$ dependence leads to a stronger amplification of SSH mapping error at the low latitudes of the EQ region. The difference between the mission combinations are especially clear in these regions when short length spans are used to determine SSH slopes, leading to a similar amplification of SSH mapping error. Since spatial scales are fairly large in the EQ region, remarkably high accuracy can be obtained there in both components when long smoothing spans (300 km) are employed, thereby effectively reducing the above effects. Because of the more unfavorable error budgets involved, the Jason-Envisat-GFO combination is not expected to lead to higher velocity accuracies than a T/P-Jason tandem mission. For all combinations velocity errors become comparable to the case with no data errors if longer spans are used, leading to almost complete removal of SSH mapping errors, but simultaneously to an increase of the total error due to the increasingly dominating effect of the attenuation of the signal.

5. Applications of Velocity Estimates From Multiple-Mission Altimetry

[40] Even though the resolution with which the mesoscale velocity field can be determined will remain limited until the launch of a dedicated high-resolution ocean topography mission, improvements with respect to single-satellite missions can be obtained from any multiple satellite combination. For example, the verification of theories for oceanic Rossby wave propagation speeds has been suggested as an important application of an interleaving T/P-Jason tandem mission. *Ducet et al.* [2000] and *Ducet and Le Traon* [2001], use merged T/P and ERS data to investigate the quality and characteristics of global velocity maps, and of

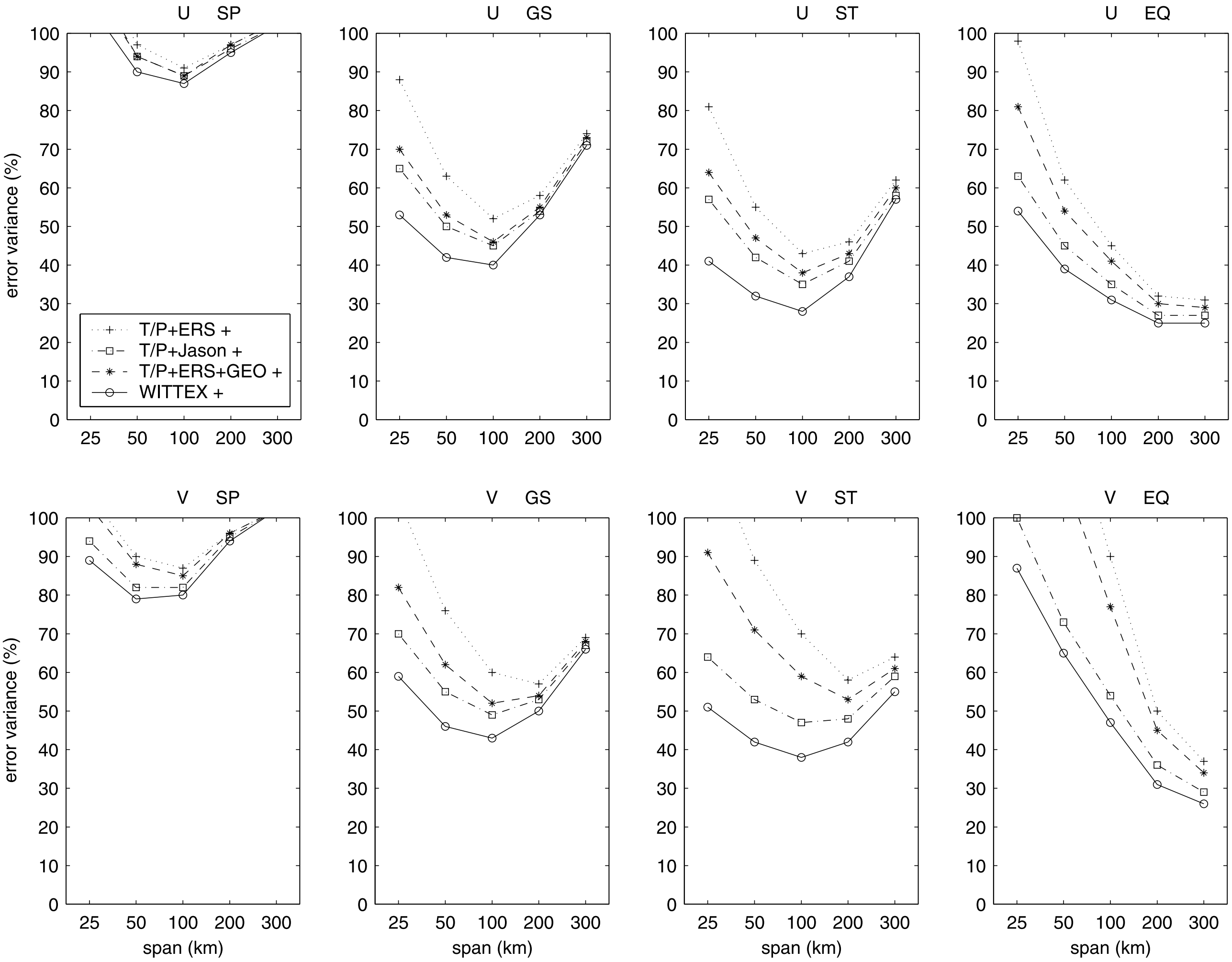

Figure 8. As in Figure 7 but for data containing realistic instrument noise and orbit errors as described in the text.

eddy kinetic energy (EKE) and Reynolds stresses in western boundary regimes, respectively. The EKE is a measure of the degree of variability and may identify regions with highly variable phenomena such as baroclinic eddies, upwelling, current meanders, waves, and overflows. The eddy field acts to accelerate or decelerate the mean flow through horizontal momentum flux convergence or divergence, as quantified by the spatial gradients of the Reynolds stress tensor components.

[41] The cross-covariance term $\langle u'v' \rangle$ of the Reynolds stress tensor, as it results from the model solution, is depicted by the contours in Figure 9 for a small area of the Gulf Stream Extension. Velocity sampling locations resulting from parallel track and crossover procedures are superimposed. (If one chooses to apply the parallel track method to an interleaved configuration one can also obtain velocity estimates along ground tracks interleaving those depicted in the second panel of Figure 9. As discussed earlier, however, the accuracy for a large track separation would be low in most regions.) The spatial scale of the cross-covariance term is seen to be fairly small. In fact, neither one of the two sample distributions appears to be able to capture all large-amplitude, small spatial scale features of the stress field consistently. The resolution with which the two-dimensional velocity field can be mapped from the crossovers may be higher but will still only capture a fraction of the wave number space occupied by the stress field.

[42] The extent to which horizontal momentum fluxes can be reproduced is investigated in Figures 10a and 10b depicting the $\langle u'u' \rangle$ and $\langle v'v' \rangle$ terms of the stress tensor as a function of longitude and latitude respectively, for an area located around the Gulf Stream core. The spatial gradients $\langle u'u' \rangle_x$ and $\langle v'v' \rangle_y$ were found by *Ducet and Le Traon* [2001] to be the largest terms contributing to zonal and meridional acceleration of the mean current respectively. The stress estimates displayed in Figures 10a and 10b are $5° \times 1°$ (lat $\times$ lon) and $1° \times 5°$ (lat $\times$ lon) averages respectively and are obtained from three separate calculations. The parallel track method was applied to a tandem configuration with a 0.75° track separation while the crossover and optimal interpolation methods were applied to an interleaved configuration. The SSH data included 2 cm noise and orbit errors (a 3 cm orbit error was added before applying the parallel track method to represent a worst-case scenario). In all three cases the stresses are underestimated but show the correct general tendencies. The optimal interpolation results are smoother than those from the other two methods which may be more strongly affected by small scale effects and outliers because

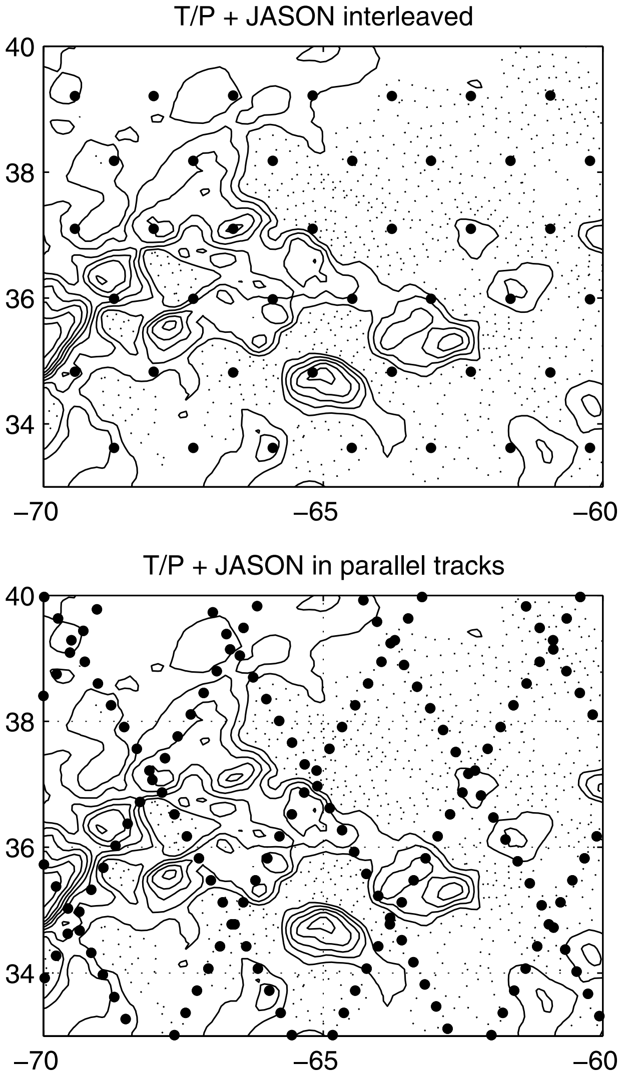

Figure 9. Velocity sample distribution for interleaving and parallel track configurations, overlayed on the $\langle u'v' \rangle$ term of the Reynolds stress tensor near the Gulf Stream core. The contour interval is 200 m^2/s^2, and negative contours are dotted.

of the more sparse distribution of velocity estimates. It is not obvious, however, that the interleaved orbit configuration leads to better results than the configuration with 0.75° track separation. In fact, the latitudinal change of $\langle v'v' \rangle$ appears to be captured most accurately in the results from the latter configuration. A 1.5° track separation was found to lead to a further underestimation of the stresses, in agreement with Figure 1. Results for $\langle u'v' \rangle$ lead to similar conclusions (not shown).

[43] Other important applications of altimetric velocities include the estimation of velocity wave number spectra and covariance functions, and the monitoring of boundary currents. These applications are discussed in reference to Figure 11, showing the spatial and temporal distribution of crossover and parallel track velocity samples along a descending track crossing the Gulf Steam Extension between 64°W and 58°W longitude. When considering samples along a single track, two main differences can be noted between the two sampling strategies. First of all, while the parallel track estimates can be considered instantaneous for all purposes, there are significant temporal offsets between crossover samples along a single track (if the midtime between over flights is used). Second, while the along-track density for a parallel track configuration is equal to that of SSH, the sampling density is much lower for the crossover application, thus limiting the resolution of the wave number spectrum and covariance function. Another advantage of high-density along-track sampling is that it is able to capture all the small-scale jets and meanders in a section across the Gulf Stream. It does so at regular zonal intervals along the mean eastward directed section of the current and therefore allows for the monitoring of transport changes over time and along the mean path.

[44] Apart from sampling considerations, the applicability of velocity estimates may depend on the impact of data errors, in particular orbit errors. Orbit errors will limit the accuracy of individual velocities obtained from a parallel track procedure as described before. It can be shown however that velocity estimates will be affected in a nearly identical way over mesoscale distances. This can be deduced from the equations for the two velocity components. Following the notation of *Stammer and Dieterich* [1999],

$$u' + \Delta u' = -\frac{g}{f}\frac{(\eta_1 + \Delta\eta - \eta_2)}{D},$$
$$v' + \Delta v' = \frac{g}{f}\frac{(\eta_3 + \Delta\eta - \eta_4)}{D'},$$

where $\Delta\eta$ is the bias between the two tracks. If $D \approx D'$, then $\Delta v' = -\Delta u' = (g/f)\ \Delta\eta/D$. The errors in the zonal and

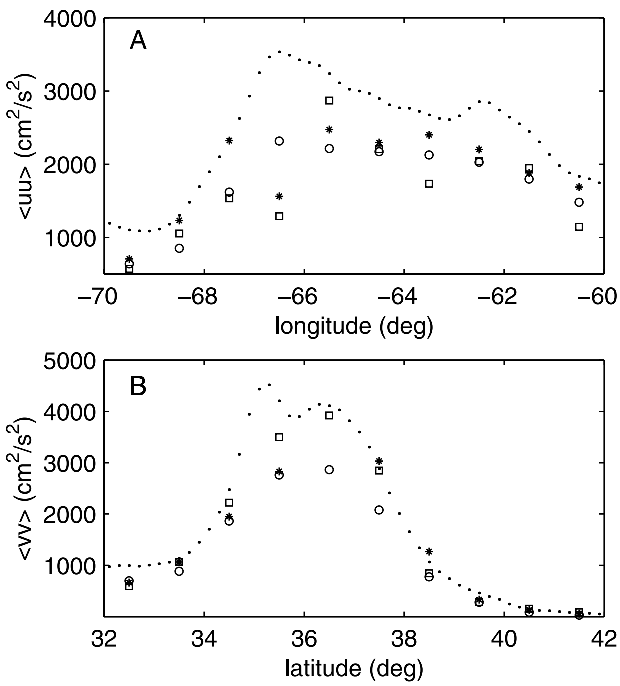

Figure 10. A comparison of the $\langle u'u' \rangle$ and $\langle v'v' \rangle$ terms of the Reynolds stress tensor, along and across the Gulf Stream core, respectively, obtained from parallel track (squares) and interleaving configurations, in the latter case obtained with both the crossover (stars) and optimal interpolation (circles) methods. The dotted line represents the model truth.

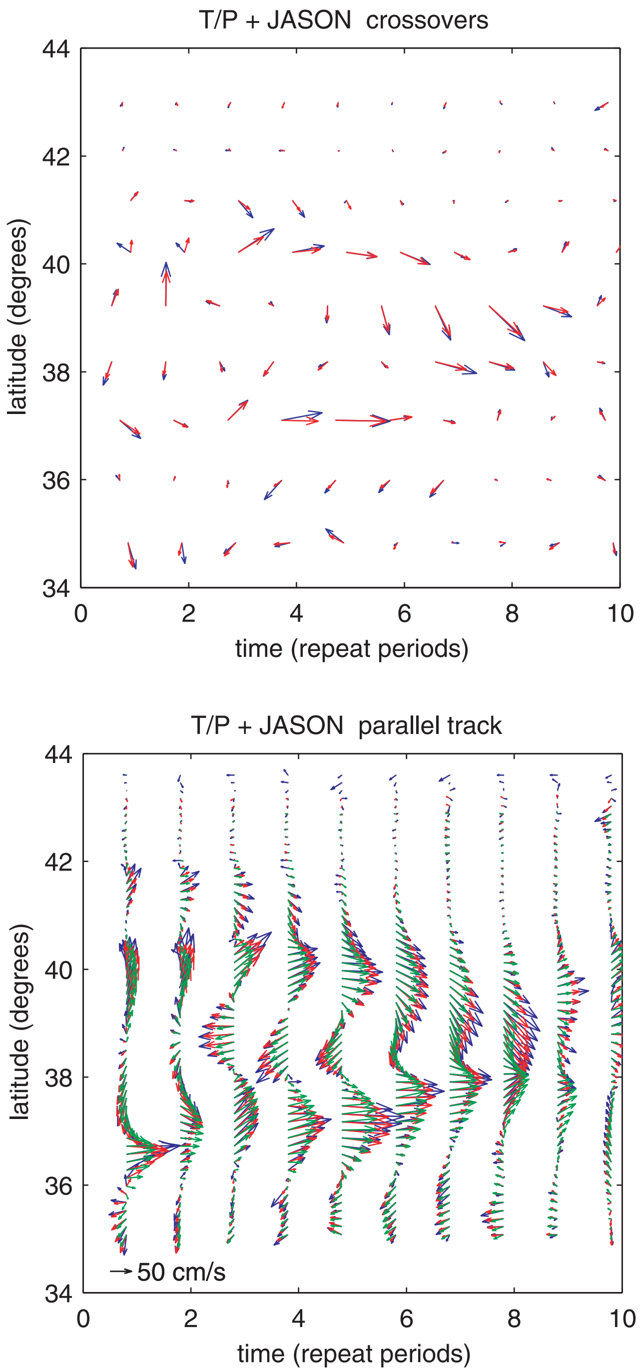

Figure 11. Velocity vectors obtained from crossover and parallel track procedures along a ground track crossing the Gulf Stream. The model velocity is shown in blue, and optimal estimates from simulated data with errors are shown in red. The green velocities were obtained by applying the parallel track method to an interleaved configuration.

meridional velocity components are obtained by rotation over $\gamma = \alpha - i$, with $\alpha = 45°$ and i the azimuth of the ground track,

$$\Delta\tilde{u} = \Delta u' \cos\gamma - \Delta v' \sin\gamma = -\frac{\Delta\eta g}{Df}(\cos\gamma + \sin\gamma),$$

$$\Delta\tilde{v} = \Delta u' \sin\gamma + \Delta v' \cos\gamma = \frac{\Delta\eta\, g}{Df}(\cos\gamma - \sin\gamma).$$

Both the orbit errors $\Delta\eta$ and the parameters in the functions on the right hand side are smooth functions of latitude with typical length scales far greater than that of the mesoscale variability. $\Delta\eta$ can be removed to first order by a mean or trend fitted to the along-track SSH on both tracks. Even though orbit errors may limit the absolute accuracy of individual estimates, covariance functions and wave number spectra computed from velocities obtained along a track will thus not be significantly corrupted by orbit errors.

[45] Estimates of transport variability may be effected by time dependency of velocity biases. For example, if the SSH bias $\Delta\eta$ changes from one repeat to the next, as may be expected, this will translate into a nonexistent change in transport over this period. One way to detect such time dependent biases in the velocities could be to use crossovers on the same track on both sides of the jet (to the north and south in this case). Assuming that crossover velocities are not affected by bias, these can help determine and remove the along-track bias in the parallel track velocities and thereby obtain temporally consistent velocity estimates. Thus neither the magnitude nor the time variability of long-wavelength SSH biases (such as orbit errors) should limit the applicability of parallel track procedures.

6. Summary and Conclusions

[46] The purpose of this paper has been to evaluate the uncertainties associated with methods to estimate surface geostrophic velocity from altimetric SSH measurements, and discuss the impact of data errors and orbit configurations. Two of these methods, crossover analysis and optimal interpolation, are currently in use, while a third method, the parallel track method, has been proposed for mission configurations involving multiple satellites in orbits with a small zonal offset.

[47] The performance of all three methods is affected in part by the sampling limitations imposed by the orbit configuration, resulting in what has been referred to here as sampling errors. The addition of data errors further impacts the accuracy of velocity estimates and introduces the need for noise reduction schemes. A side effect of this smoothing is the attenuation of the velocity signal. For all three methods optimal smoothing parameters need to be chosen that minimize the combined impact of sampling and data error. These optimal parameters in turn may depend on the region of interest because of the variation of spatial and temporal scales of signal variability. The use of multiple altimetric satellites would enable more efficient orbit error reduction schemes based on crossover minimization than would be possible for any single satellite. Such schemes have not been employed in this paper but may allow the consideration of more optimistic error budgets than have been estimated for individual missions. This is an area where more research is warranted.

[48] The parallel track method, recently proposed for the explicit purpose of velocity determination, is found to be capable of producing useful estimates in subtropical and midlatitude ocean regions for a 0.75° track separation if the orbit error is 2 cm or less. Application of this method near the turning latitude and near the equator will be feasible for 1 cm orbits while accuracies obtained in regions of strong signal variability, such as the Gulf Stream and North

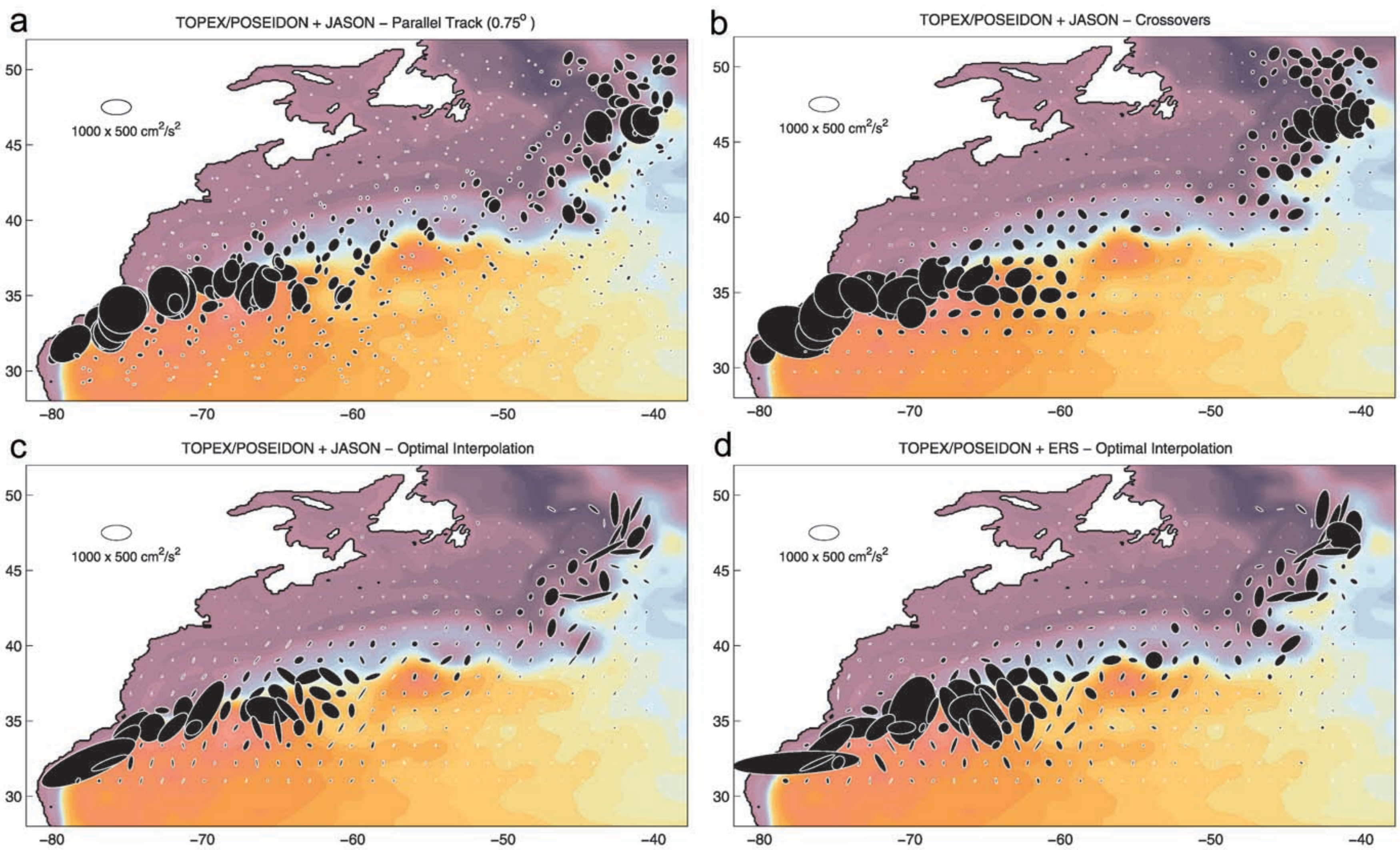

Figure 12. Error variance ellipses for four different mission configurations and methods, obtained from simulated SSH samples including data errors as used in the text. Only every sixteenth along-track point from the parallel track estimates, and every fourteenth point in zonal and meridional directions from the optimal interpolated grid are displayed.

Table 1. Comparison of Velocity Error Variances, Expressed as a Percentage of Signal Variance, for the Region 34°–39°N, 70°–60°W, for Different Missions and Estimation Methods[a]

Missions	Method	*U*, %	*V*, %
T/P + Jason (0.75°)	PT	13	11
T/P + Jason (1.5°)	PT	44	34
T/P	XO	8	16
Geosat	XO	10	33
ERS	XO	34	127
T/P + ERS	OI	27	36
T/P + ERS + Geosat	OI	21	25
T/P + Jason	OI	22	26
WITTEX(3)	OI	19	21

[a] Data errors are described in the text.

Atlantic Current, are of the same order as those of crossover velocities, and better than can be obtained from optimal interpolation, even for 3 cm orbit errors. Only in the subtropical gyre can crossover velocities be obtained with high accuracy simultaneously in both components, even for the most optimal noise budgets. This is primarily due to the latitude dependence of the crossover angle which tends to amplify noise in one of the two components at very low and high latitudes. For a T/P-class altimeter the lowest achievable velocity error variance is about 20% of the signal variance for the *U* component and about 40% for the *V* component, when averaged over a large region. After determining the optimal span of the slope fit, and thereby the extent of smoothing of the velocity, it was found that accuracies of velocities obtained from optimal interpolation products are slightly lower when averaged over regions of high variability such as the Gulf Stream. An advantage however is that, unlike the other two methods, useful velocities can be obtained at all latitudes, with comparable accuracy in the two components. In this paper an interleaving T/P-Jason tandem mission, as well as three alternative mission combinations were considered. It was found that the accuracy of velocity estimates from coordinated missions is in general higher than that from uncoordinated missions, with the relative performance of different satellite combinations being in agreement with results from studies of formal mapping errors. The magnitude of data errors becomes important primarily in low-variability and low-latitude regions.

[49] Velocity errors have been presented as fractions of signal variance. In order to give an impression of the absolute magnitudes of these errors, Figure 12 presents error variance ellipses for the Gulf Stream region for some of the configurations and methods considered in this paper. The ellipses are superimposed on the model mean sea surface field to help locate the mean position of the Gulf Stream's core. Absolute errors are seen to be very much larger close to the core, due to the increased velocities and variability there. As shown in Table 1, however, relative errors in this region are actually much smaller than in the more quiet regions away from the core. For the T/P-Jason tandem mission configuration, velocity error variances within the actual Gulf Stream core are found to be below 20% of signal variance when estimated at crossovers or between parallel tracks, and below 30% when estimated from optimal interpolation, lower than the averages over the entire GS region.

[50] Consideration of the sampling distributions resulting from two interleaving or parallel orbits suggests that different scientific applications may benefit considerably from either configuration. The more homogeneous spatial distribution of SSH samples resulting from two interleaving orbits means that SSH maps can be obtained with a higher resolution. Velocities estimated from such maps however, are not necessarily more accurate than those estimated from alternative methods as discussed here. In fact, it appears that two (or more) altimeters positioned in slightly offset orbits (≈0.75°), and with reduced orbit errors, may lead to more accurate velocities and to a range of interesting scientific applications. While different scientific questions can be addressed depending on the configuration of only two conventional altimeters, a dedicated high-resolution altimetry mission would enable the advancement of all these science questions.

[51] **Acknowledgments.** We are grateful to Rick Smith for providing the model fields. Valuable discussions with Dudley Chelton and Lee-Lueng Fu are highly appreciated. The manuscript was much improved after comments from the two reviewers. This work was supported in part through contract 1205624 with the Jet Propulsion Laboratory.

References

Chelton, D. B., J. C. Ries, B. J. Haines, L.-L. Fu, and P. S. Callahan, Satellite altimetry, in *Satellite Altimetry and the Earth Sciences*, edited by L.-L. Fu and A. Cazenave, pp. 1–131, Academic, San Diego, Calif., 2001.

Cleveland, W. S., and S. J. Devlin, Locally weighted regression: An approach to regression analysis by local fitting, *J. Am. Stat. Assoc.*, *83*, 596–610, 1988.

Ducet, N., and P. Y. Le Traon, A comparison of surface eddy kinetic energy and Reynolds stresses in the Gulf Stream and the Kuroshio Current systems from merged TOPEX/Poseidon and ERS-1/2 altimetric data, *J. Geophys. Res.*, *106*, 16,603–16,622, 2001.

Ducet, N., P. Y. Le Traon, and G. Reverdin, Global high resolution mapping of ocean circulation from TOPEX/Poseidon and ERS-1/2, *J. Geophys. Res.*, *105*, 19,477–19,498, 2000.

Fu, L.-L., (Ed.), Minutes of the third joint TOPEX/Poseidon and Jason-1 science working team meeting, Nov 15–17, 2000, Miami Beach, Florida, *JPL Rep. D-20240*, Miami Beach, Fla., 2000.

Greenslade, D. J., D. B. Chelton, and M. G. Schlax, The midlatitude resolution capability of sea level fields constructed from single and multiple satellite altimeter datasets, *J. Atmos. Oceanic Technol.*, *14*, 849–870, 1997.

Høyer, J. L., D. Quadfasel, and O. B. Andersen, Subsurface processes detected with satellite altimetry, *Can. J. Remote Sens.*, in press, 2002.

Knudsen, P., Altimetry for Geodesy and Oceanography. in *Geodesy and Geophysics: Lecture Notes for the NKG Autumn School 1992*, edited by J. Kakkuri, *Publ. Finn. Geod. Inst. 115*, Helsinki, 1993.

Kuragano, T., and M. Kamachi, Global statistical space-time scales of oceanic variability estimated from the TOPEX/Poseidon altimeter data, *J. Geophys. Res.*, *105*, 955–974, 2000.

Le Traon, P. Y., and G. Dibarboure, Mesoscale mapping capabilities of multiple-satellite altimeter missions, *J. Atmos. Oceanic Technol.*, *15*, 1208–1223, 1999.

Le Traon, P. Y., G. Dibarboure, and N. Ducet, Use of a high-resolution model to analyze the mapping capabilities of multiple-altimeter missions, *J. Atmos. Oceanic Technol.*, *18*, 1277–1288, 2001.

Morrow, R., R. Coleman, J. Church, and D. Chelton, Surface eddy momentum flux and velocity variances in the Southern Ocean from Geosat altimetry, *J. Phys. Oceanogr.*, *24*, 2050–2071, 1994.

Parke, M. E., R. L. Stewart, D. L. Farless, and D. E. Cartwright, On the choice of orbits for an altimetric satellite to study ocean circulation and tides, *J. Geophys. Res.*, *92*, 11,693–11,707, 1987.

Raney, R. K., The delay Doppler radar altimeter, *IEEE Trans. Geoscience Remote Sens.*, *36*, 1578–1588, 1998.

Raney, R. K., and D. L. Porter, WITTEX: An innovative multi-satellite radar altimeter constellation, in *Report of the High-Resolution Ocean topography Science Working Group Meeting*, edited by D. B. Chelton, *Rep. 2001-4*, Coll. of Oceanic and Atmos. Sci., Oregon State Univ., Corvallis, 2001.

Ray, R., and G. Mitchum, Surface manifestation of internal tides generated near Hawaii, *Geophys. Res. Lett.*, *23*, 2101–2104, 1996.

Rodriguez, E., B. D. Pollard, and J. M. Martin, Wide-swath ocean altimetry using radar interferometry, *IEEE Trans. Geoscience Remote Sens.*, in press, 2002.

Schlax, M. G., and D. B. Chelton, Frequency domain diagnostics for linear smoothers, *J. Am. Stat. Assoc.*, *87*, 1070–1081, 1992.

Smith, R. D., M. E. Maltrud, F. O. Bryan, and M. W. Hecht, Numerical simulation of the North Atlantic Ocean at 1/10°, *J. Phys. Oceanogr.*, *30*, 1532–1561, 2000.

Stammer, D., Global characteristics of ocean variability estimated from regional TOPEX/Poseidon altimeter measurements, *J. Phys. Oceanogr.*, *27*, 1743–1769, 1997.

Stammer, D., and C. Dieterich, Space-borne measurements of the time-dependent geostrophic ocean flow field, *J. Atmos. Oceanic Technol.*, *16*, 1198–1207, 1999.

Stammer, D., C. Wunsch, and R. Ponte, De-aliasing of global high frequency barotropic motions in altimeter observations, *Geophys. Res. Lett.*, *27*, 1175–1178, 2000.

Strub, P. T., T. K. Chereskin, P. P. Niiler, C. James, and M. D. Levine, Altimeter-derived variability of surface velocities in the California Current System, 1, Evaluation of TOPEX altimeter velocity resolution, *J. Geophys. Res.*, *102*, 12,727–12,748, 1997.

Vincent, P., and E. Thouvenot, Status of Ka-band altimetry, in *Report of the High-Resolution Ocean Topography Science Working Group Meeting*, edited by D. B. Chelton, *Rep. 2001-4*, Coll. of Oceanic and Atmos. Sci., Oregon State Univ., Corvallis, 2001.

Willebrand, J., R. H. Käse, D. Stammer, H.-H. Hinrichsen, and W. Krauss, Verification of Geosat sea surface topography in the Gulf Stream Extension with surface drifting buoys and hydrographic measurements, *J. Geophys. Res.*, *95*, 3007–3014, 1990.

Wunsch, C., and D. Stammer, Satellite altimetry, the marine geoid, and the oceanic general circulation, *Ann. Rev. Earth Planet. Sci.*, *26*, 219–253, 1998.

O. Leeuwenburgh and D. Stammer, Scripps Institution of Oceanography, University of California, San Diego, 9500 Gilman Drive, La Jolla, CA 92093-0230, USA. (oleeuwenburgh@ucsd.edu)